

1
2
3
4
5
6
7
8
9
10

Original Research Article

Remote Sensing Based Land Surface Temperature Analysis in Diverse Environment of Lalgudi Block

ABSTRACT

Introduction: Land Surface Temperature (LST) is a significant climatic variable and defined as how hot the "surface" of the Earth would feel to the physical touch in a particular location. A spatial analysis of the land surface temperature with respect to different land use/cover changes is vital to evaluate the hydrological processes.

Methods: The objective of this paper is to assess the spatial variation of land surface temperature derived from thermal bands of the Landsat 8 Operational Land Imager (OLI) and the Thermal Infrared Sensor (TIRS) by using split window algorithm.

Place and Data: The study was conducted in Lalgudi block of Trichy District, Tamil Nadu, India. The block has diverse environment like forest area, barren land, river sand bed, water bodies, dry vegetation, cultivated areas (paddy, sugarcane, banana etc.) and settlements. Landsat 8 satellite images for four selected scenes (December 2014 & January 2015 and December 2017 & January 2018) were used to estimate the LST.

Results: The spatial and temporal variation of Normalized Difference Vegetation Index (NDVI) and LST were estimated. The average NDVI values of cropped fields varied from 0.3 to 0.5 in all the scenes. The maximum value of LST ranging from 35 to 40°C was recorded in river sand bed. Subsequently, semi-urban settlements in the central part of Lalgudi block exhibited higher temperature ranging from 28 – 30°C. The LST of paddy crop and sugarcane was in the range of 23 to 25°C. The water bodies exhibited LST around 20°C. The coconut plantations, forest area and *Prosopis juliflora* showed LST value ranging from 24 – 29°C. This kind of block level monitoring studies helps in adopting suitable policies to overcome or minimize the problems triggered by increase in land surface temperature.

Keywords: Land Surface Temperature; Normalized Difference Vegetation Index; Land use/cover

1. INTRODUCTION

Land Surface Temperature (LST) is a significant climatic variable and defined as how hot the "surface" of the Earth would feel to the physical touch in a particular location. It is the skin temperature of the earth surface that depends on the amount of sunlight received by any geographical area. Apart from sunlight, LST is also affected by the land cover, which leads to change in land surface temperature. The variations in land surface heat fluxes affect the ecological environment and hydrological processes [1]. It also has a direct impact on vegetation of that location.

11
12
13
14
15
16
17
18
19
20
21
22
23

24 LST plays a direct role in estimating long wave fluxes and an indirect role in estimating latent
25 and sensible heat fluxes [2]. Soil moisture estimation [3] and evapotranspiration modeling [4]
26 can be done based on LST for estimating the crop water requirement and planning efficient
27 water management strategies in a regional scale. Hence knowledge on spatial and temporal
28 variation of LST is essential.

29 With the advent of satellite images and digital image processing techniques, now it is
30 possible to calculate spatial variation of LST. Landsat 8 satellite images comes with two
31 different sets of images that are from Operation Land Imager (OLI) sensor with nine bands
32 (band 1 to 9) and Thermal Infrared sensor (TIRS) with two bands (band 10 and 11) [5].
33 These images helps in mapping spatial extent, land surface temperature, vegetation cover
34 and chemical composition of the surface.

35 Many researchers used different algorithms to estimate LST from remote sensing images [6]
36 such as Split-Window algorithm (SW), Dual Angle algorithm (DA), Single-Channel algorithm
37 (SC). An attempt was made to detect the change of land surface temperature in relation to
38 land use land cover change and fractal vegetation cover in some selected phases at English
39 Bazar Municipality of Malda, West Bengal, India [7]. And also investigated the temperature
40 characters in different vegetation density zones, water depths, built up zones over selected
41 time periods. A study was conducted to assess the impact of land cover change (LCC) on
42 LST, using Landsat TM 5, Landsat 8 TIRS/OLI and Digital Elevation Model (ASTER) for Spiti
43 Valley, Himachal Pradesh, India [8]. Land surface temperature in relation to Land use types
44 and geological formation in northeast Jordan using split-window algorithm was estimated [9].
45 A review about the progress in estimation of LST from TIR and suggested directions for
46 future research on the subject was presented [10].

47 This study attempts to analyze the spatial variation of land surface temperature by using
48 split-window algorithm from Landsat 8 satellite images for various land use/cover in Lalgudi
49 block.

50 **2. MATERIAL AND METHODS**

51

52 **2.1 Study Area**

53 Lalgudi block, located at Tiruchirapalli District, Tamil Nadu, India was selected for this study.
54 The geographical location of Lalgudi block is shown in Figure 1. The northern part of Lalgudi
55 block has dense dry vegetation and barren lands. The southern part is bounded by River
56 Coleroon. The Lalgudi Town is located at the central part of the block. Most of the inner part
57 of the Lalgudi has cultivated areas where paddy, sugarcane, banana and other vegetables
58 are grown.

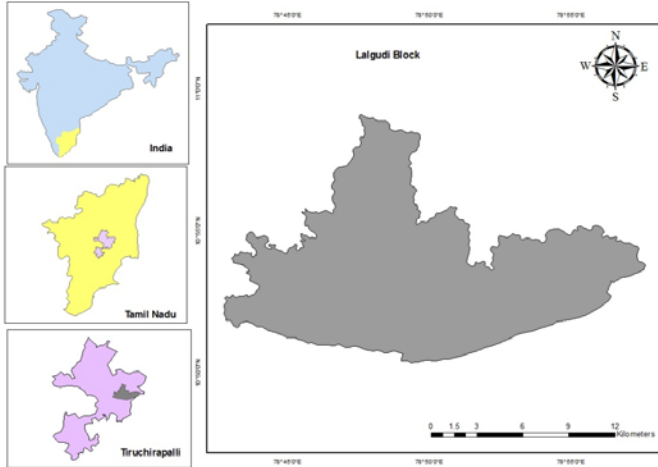


Fig. 1: The Location of study area – Lalgudi Block

2.2 Image Selection

Landsat 8 is the most recently launched satellite of the Landsat series. The Landsat 8 satellite images were downloaded from the USGS Earth Explorer website. To maintain homogeneity in dataset, two pairs of images of December 05, 2014 & January 22, 2015 and December 29, 2017 & January 30, 2018 were acquired. The period of images taken was based on paddy cultivation season. Table 1 presents image acquisition date, solar elevation angle and zenith angle for the Landsat 8 data products used. The images were selected such that there is no or minimum cloud cover (table 1) in order to avoid error.

Table 1: Meta Data of Landsat 8 image used

S. No.	Acquisition Date (yyyy/mm/dd)	Solar Elevation Angle (degrees)	Solar Azimuth Angle (degrees)	Cloud Cover in image (%)	Cloud Cover in study area (%)
1	2014-12-05	49.38	146.60	2.46	0.77
2	2015-01-22	48.22	138.31	0.01	0.00
3	2017-12-29	47.08	144.18	23.15	0.40
4	2018-01-30	49.39	135.62	0.17	0.00

2.3 Computation of Land Surface Temperature (T_s)

Land Surface temperature (T_s) is an important parameter in understanding the exchange of energy between the earth surface and the environment. LST was calculated from the thermal band (band 10 and 11) radiance values of the Landsat 8 image. The equation for estimation of surface temperature is as follow:

$$T_s = \frac{K_2}{\ln \left(\frac{\varepsilon_s * K_1}{\rho_b} \right)} \quad (1)$$

77 The radiance ρ_b of the thermal band (band 10) was calculated from Equation 2. The
 78 constants K_1 and K_2 for band 10 are 774.8853 and 1321.0789 which was taken from the
 79 metadata file. The surface emissivity (ϵ_s) was calculated from equation 3. The radiance (ρ_b)
 80 was calculated from the pixel values of different bands (DN_b) using the following equation:

$$81 \quad \rho_b = Add_{rad,b} + (Mult_{rad,b} * DN_b) \quad (2)$$

82 where $Add_{rad,b}$ is additive and $Mult_{rad,b}$ is multiplicative terms related to different band
 83 radiance. The values of Add_{rad} and $Mult_{rad}$ terms of band 10 are 0.10000 and 3.3420E-04.

84 Surface emissivity (ϵ_s) is the ratio of the thermal energy radiated by the surface to the
 85 thermal energy radiated by a blackbody at the same temperature. It is given by:

$$86 \quad \epsilon_s = \begin{cases} 1.009 + 0.047(\ln(NDVI)) \rightarrow (NDVI > 0) \\ 1 \rightarrow (NDVI < 0) \end{cases} \quad (3)$$

87 Thus the surface emissivity was empirically derived from NDVI. NDVI is the ratio of
 88 difference in reflectivity of near-infrared (NIR) band and red band to their sum. The
 89 expression for estimation of NDVI is given by

$$90 \quad NDVI = \frac{NIR - RED}{NIR + RED} \quad (4)$$

91 In Landsat 8 image, the near infrared is band 5 and the red is band 4. Using Raster
 92 Calculator tool in ArcGIS, NDVI raster was obtained.

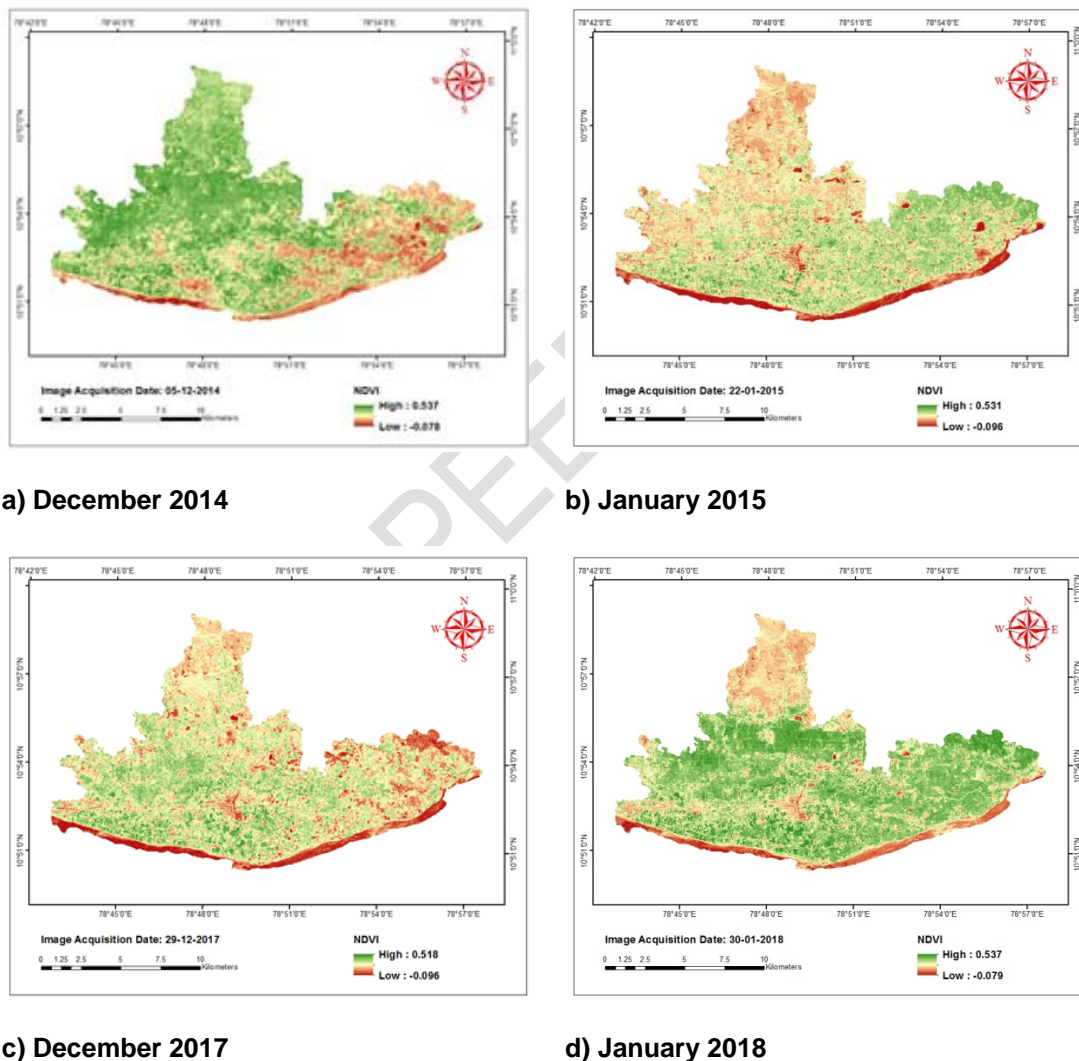
93 A ground truth survey was conducted to identify different land use/cover in Lalgudi block.
 94 The variation of LST were compared graphically for each land use/cover.

95 **3. RESULTS AND DISCUSSION**

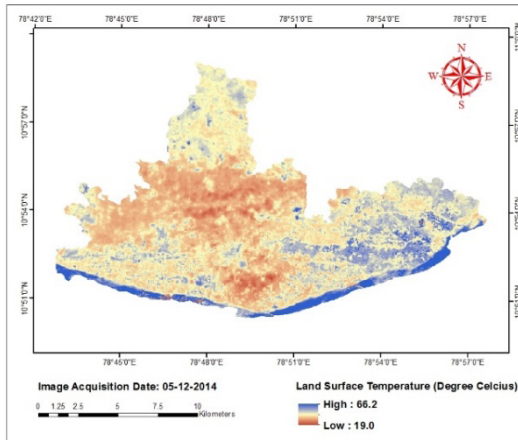
96
 97 The spatial and temporal variation of NDVI and LST are presented in Figure 2 and 3
 98 respectively for the four selected scenes. The southern part of the study area is bounded by
 99 the River Coleroon and hence negative values of NDVI was observed in the southern part of
 100 all the scenes (Fig. 2). The NDVI values for water bodies ranges from -0.07 to -0.09. The
 101 river sand bed and standing water in the pits resulted in negative values of NDVI in the
 102 southern part. Subsequently, the LST was higher in the river sand bed and comparatively
 103 lesser in the pits with standing water. This is clearly indicated in the images by pale yellow
 104 color patches in the southern part of LST maps (Fig. 3). Similarly, the LST was higher in the
 105 northern part (Fig. 3) where barren land and dry vegetation exists. The dry vegetation
 106 includes cactus, prosopis etc. Likewise fallow land exhibited a maximum LST (29.2 °C) in the
 107 study conducted at Malda [7]. The LST value of a lake located in the eastern part of Lalgudi
 108 was around 20°C when water is available (Fig. 3a and 3b). The LST increased in December
 109 2017 (Fig. 3c) and January 2018 (Fig. 3d) images because of the presence of water weeds
 110 on the surface of water. The value of NDVI also simultaneously increased for the lake in
 111 those respective scenes (Fig. 2c and 2d). It was reported that the LST of water bodies was
 112 higher compared to LST of water hyacinth [7].

113 The scenes used in this study falls in the active tillering (December 2017), panicle initiation
 114 (December 2014 and January 2018) and dough stage (January 2015) of samba season
 115 paddy crop respectively. In all stages of paddy, the LST was in the range of 23 to 25 °C.
 116 Similarly LST of sugarcane was also in the range of 23 – 25 °C. The average NDVI values of
 117 sugarcane and banana fields varied from 0.3 to 0.5 in all the scenes.

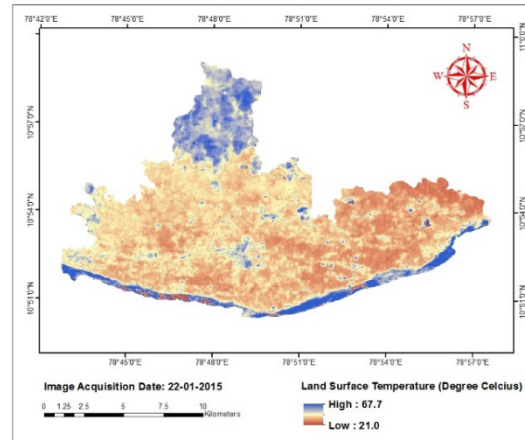
118 In December 2017 and January 2018 scenes, the LST of Banana was comparatively higher
 119 than LST in December 2014 and January 2015 scenes (Fig. 4) because, in December 2017
 120 and January 2018, there existed newly planted banana plants. The combined effect of soil
 121 and young banana plants was the reason behind the increase in LST. The coconut
 122 plantations, forest area and *Prosopis juliflora* exhibited similar trend (Fig. 4) of LST value
 123 ranging from 24 – 29 °C. This was greater when compared to LST of the paddy crop.



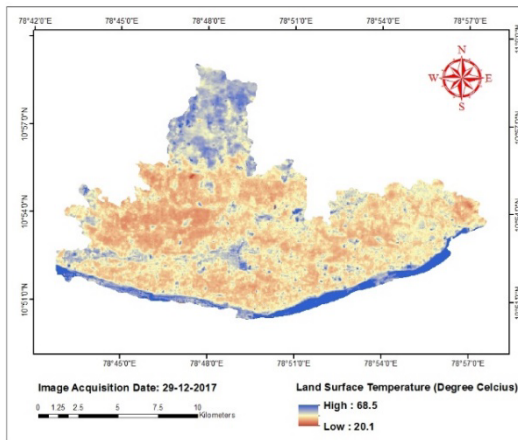
124 **Fig. 2: Spatio-Temporal Variation of NDVI in Lalgudi Block**



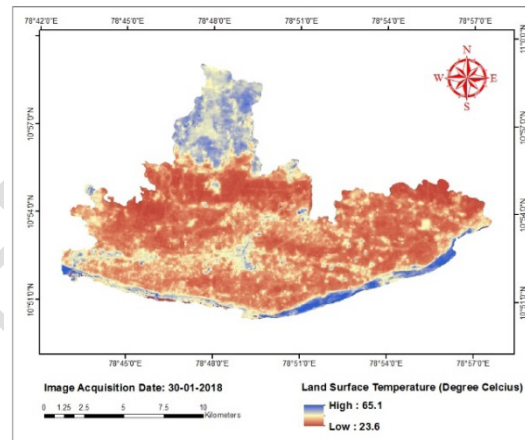
a) December 2014



b) January 2015

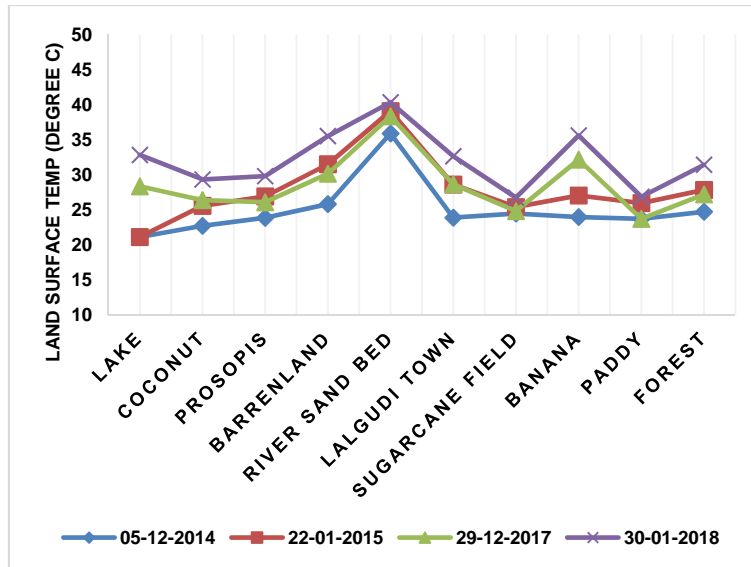


c) December 2017



d) January 2018

125 Fig. 3: Spatio-Temporal Variation of LST in Lalgudi Block



126

127 **Fig. 4: LST Variation of Different Surfaces in Lalgudi Block**

128 The semi-urban settlements in the central part of Lalgudi block exhibited higher temperature
 129 (28 – 30°C) compared to the cropped surface. It was also reported that a dominant built up
 130 land experienced LST greater than 31.5 °C [7]. The maximum value of LST ranging from 35
 131 to 40 °C was recorded in the river sand bed. Similarly it was noticed that asphalt and
 132 concrete gave the highest surface temperatures, while vegetated surfaces gave the lowest
 133 [11]. Bare soil gave surface temperatures that lie between those for pavements and plant-
 134 covered surfaces [11].

135 **4. CONCLUSION**

136

137 A mathematical approach was used to estimate the LST from brightness temperature
 138 calculated from thermal bands of TIRS sensor and land surface emissivity and NDVI derived
 139 from optical bands of OLI sensor. LST was diversified due to positional influence of the
 140 existing land use/cover of Lalgudi block. A discrete difference in LST was identified in
 141 different land use/cover. The transformation of wetland into urban land, exchange of land
 142 between orchard and agricultural land etc. are some vital causes behind land surface
 143 temperature change which may be avoided. Green belt can be implemented in the areas
 144 having higher land surface temperature. This kind of block level monitoring studies helps in
 145 adopting suitable policies to overcome or minimize the problems triggered by increase in
 146 land surface temperature. Crop water requirement and efficient water management studies
 147 in a regional scale can also be done through the spatial assessment of land surface
 148 temperature.

COMPETING INTERESTS

"Authors have declared that no competing interests exist."

AUTHORS' CONTRIBUTIONS

All authors equally contributed.

CONSENT

"All authors declare that 'written informed consent was obtained from the patient (or other approved parties) for publication of this case report and accompanying images. A copy of the written consent is available for review by the Editorial office/Chief Editor/Editorial Board members of this journal.'"

ETHICAL APPROVAL

"No human or animals are harmed in this study"

REFERENCES

- [1] Hu, G., Zhao, L., Wu, R. L. X., Wu, T., Zhu, X., Pang, Q., Liu, G.Y. and Du, E. 2019. Simulation of land surface heat fluxes in permafrost regions on the Qinghai-Tibetan Plateau using CMIP5 models. *Atmospheric Research*.
- [2] Bastiaanssen, W. G. M., Menenti, M., Feddes, R. A., Holslag, A. A. M. A. 1998. Remote Sensing surface energy balance algorithm for Land (SEBAL) – Formulation. *Journal of Hydrology*. 198-212.
- [3] Price, J.C. 1990. The potential of Remotely Sensed Thermal Infrared data to Infer Surface Soil Moisture and Evaporation. *Water Resources*. 16: 787-795.
- [4] Silva, B.B., Mercante, E., Boas, M.A.V., Wrublack, S.C. and Oldoni, L.V. 2018. Satellite-based ET estimation using Landsat 8 images and SEBAL model. *Revista Ciência Agronômica*. 49 (2): 221-227
- [5] Roy, D.P., Wulder, M.A., Loveland, T.R., Woodcock, C.E., Allen, R.G., Anderson, M.C., Helder, D., Irons, J.R., Johnson, D.M., Kennedy, R., Scambos, T.A., Schaaf, C.B., Schott, J.R., Sheng, Y., Vermote, E.F., Belward, A.S., Bindschadler, R., Cohen, W.B., Gao, F., Hipple, J.D., Hostert, P., Huntington, J., Justice, C.O., Kilic, A., Kovalsky, V., Lee, Z.P., Lymburner, L., Masek, J.G., McCorkel, J., Shuai, Y., Trezza, R., Vogelmann, J., Wynne, R.H. and Zhu, Z. 2014. Landsat-8: Science and product vision for terrestrial global change research. *Remote Sensing of Environment*. 145:154–172.
- [6] Latif, M.S. 2014. Land Surface Temperature Retrieval of Landsat-8 Data Using Split Window Algorithm—A Case Study of Ranchi District. *International Journal of Engineering Development and Research*, 2, 3840-3849.
- [7] Pal, S., and Ziaul, S. 2017. Detection of land use and land cover change and land surface temperature in English Bazar urban centre. *The Egyptian Journal of Remote Sensing and Space Science*, 20(1), 125–145.

- 194 [8] Kumar, P., Husain, A., Singh, R.B., and Kumar, M. 2018. Impact of land cover change
195 on land surface temperature: a case study of Spiti Valley. *Journal of Mountain Science*.
196 15(8). 1658-1670
- 197 [9] Ibrahim, M. and Abu-Mallouh, H. 2018. Estimate Land Surface Temperature in Relation
198 to Land Use Types and Geological Formations Using Spectral Remote Sensing Data in
199 Northeast Jordan. *Open Journal of Geology*, 8, 174-185
- 200 [10] Li, Z-L., Tang, B-H., Wu, H., Ren, H., Yan, G., Wan, Z., Trigo, I.F., and Sobrino, J.A.
201 2013. Satellite-derived land surface temperature: Current status and perspectives.
202 *Remote Sensing of Environment*. 131:14–37
- 203 [11] Herb, W. R., Janke, B., Mohseni, O., & Stefan, H. G. 2008. Ground surface temperature
204 simulation for different land covers. *Journal of Hydrology*, 356(3-4), 327–343.

205

206 **DEFINITIONS, ACRONYMS, ABBREVIATIONS**

207

- 208 1. Land Surface Temperature (LST)
209 2. Normalized Difference Vegetation Index (NDVI)
210 3. Split Window Algorithm (SW)
211 4. Operation Land Imager (OLI)
212 5. Thermal Infrared sensor (TIRS)